International Journal of Electrical and Computer Engineering (IJECE)
Vol. 11, No. 1, February 2020, pp. 182∼200
ISSN: 2088-8708, DOI: 10.11591/ijece.v11i1.pp182-200

Power system operation considering detailed modelling of energy storage systems

Sergio Cantillo, Ricardo Moreno
Energy and Mechanical Department, Universidad Autónoma de Occidente, Colombia

Article Info

Article history:

Received Apr 13, 2020
Revised Apr 14, 2020
Accepted May 28, 2020

Keywords:

Energy storage systems
Generation dispatch
Optimal power flow
Renewables sources

ABSTRACT

The power system operation considering energy storage systems (ESS) and renewable power represents a challenge. In a 24-hour economic dispatch, the generation resources are dispatched to meet demand requirements considering network restrictions. The uncertainty and unpredictability associated with renewable resources and storage systems represents challenges for power system operation due to operational and economical restrictions. This paper developed a detailed formulation to model energy storage systems (ESS) and renewable sources for power system operation in a DCOPF approach considering a 24-hour period. The model is formulated and evaluated with two different power systems (i.e. 5-bus and IEEE modified 24-bus systems). Wind availability patterns and scenarios are used to assess the ESS performance under different operational circumstances. With regard to the systems proposed, there are scenarios in order to evaluate ESS performance. In one of them, the increase in capacity did not represent significant savings or performance for the system, while in the other it was quite the opposite especially during peak load periods.

Corresponding Author:

Ricardo Moreno,
Energy and Mechanical Department,
Universidad Autónoma de Occidente,
Calle 25 # 115-85, Cali, Colombia.
Email: rmoreno@uao.edu.co

1. INTRODUCTION

Nowadays, the generation portfolio of electricity in power systems is more diversified than some years ago by the integration of renewable resources [1]. Environmental concerns are pushing the integration of technologies to produce electricity with renewable resources [2]. As a result, there is an increasing to spur investments in order to diminish the conventional fossil fuel-based power generation [3–5]. Consequently, the international energy agency (IEA) reports that renewable energy sources have increased at an average annual rate of 2.0 % from 1990 [6]. Growth is largely due to solar PV (37.4 %) and wind power (23.4 %) [6].

The inherent features of this type of resources as uncertainty and variability impact power system operation [7–10]. In this context, power systems require strategies to integrate such intermittent resources with flexibility to meet the demand requirements [11]. The energy storage systems (ESS) represent a technology to store renewable energy according to their availability during the day (i.e., there are high quantities of electricity from PV systems at noon). The ESS can absorb energy when generation exceeds the load especially when this surplus come from renewable sources and supply this energy to the grid during load peak hours [12, 13]. Thus, the ESS provides flexibility under the integration of renewable resources given that the power dispatch can be settled to a desirable supply profile [14, 15].

The integration of energy storage systems (ESS) represent a challenge for the operation of power systems from different perspectives. The quality and reliability can be compromised due to misuse, misplacing or bad sizing of ESS [16]. Nonetheless, other challenges for power system operation are recognized, such as performance and safety (viewed from its constituent materials, interconnections [17, 18], and service life), the distributed generation impacts in the power system coherency [19], the regulatory environment, the investment costs, and the industry acceptance [20]. These issues can occur because system operation involves decisions in different time frames (since minutes to days) including weather-dependent renewable units scheduling and their reserves [21] (e.g. wind [22]) as well as considering other related variables. However, the ESS mathematical modeling and its integration to power systems is a challenge with great impact and importance.

The optimal power flow (OPF) is used widely by power systems operators to dispatch economically the generation resources according to operational and economical restrictions [23]. From this perspective, the power system operation requires a detailed modeling of storage systems in order to be included in the OPF mathematical formulation. There are several reasons for including these energy storage models in the economic dispatch. One of them is the more efficient integration of renewable energy sources, since these devices contribute to diminish the effects of the stochastic nature of these sources [24]. Also, the ESS contribute to maintain the stability in the power system operation, due to they restrict the fluctuation of instantaneous power coming mostly from renewable sources [25, 26]. Likewise, they allow a more efficient economic dispatch since these devices provide flexibility that reduces the amount of power coming from more expensive sources (i.e., they deliver when there is a lack of energy, and store when there is a surplus), being cheaper and with less waste [27].

However, the integration of ESS's into an OPF model introduces inter alia, time interdependence. That is to say the ESS can charge in periods of high wind or low demand (i.e. is absorbing power from the grid), and discharge in periods of low wind availability or load peak (i.e is injecting power to the grid). This choice depends on the charge status (i.e. SoC) at the previous time interval and their respective efficiency. Also, technical and economical conditions are required to avoid unexpected situations as charging and discharging simultaneously. In other words, this situation implies that ESS would be paid for charging and discharging at once [11]. Among others, the dual feature of absorbing and generating power requires a precise modelling for power system operation.

This paper proposes a detailed formulation to include ESS in the optimal power flow with multiple generation sources to provide a 24-hour dispatching to meet demand requirements. Since energy storage systems could be defined as a generator and load due to the dual feature and also are time-correlated as mentioned above. The proposed formulation determines the optimal outputs for all generation portfolio as well as ESS charging/discharging schedules seen through its SoC, all of them under different operation conditions and scenarios.

The paper is organized as follows. The problem description and formulation are presented in Section 2. In Section 3, the 5-bus and IEEE 24-bus modified systems and their parameters are described. Then, the proposed procedure is tested using the systems described above. At the end of this section, the results are analyzed and discussed. Section 4 provides some concluding remarks about this topic.

- Literature review

The optimal power flow for dispatching generation resources including renewable sources has been widely discussed. The DC multi-period optimal power flow (DCOPF) formulation have been extended to include the variable nature of renewable power generation, elements such as uncertainty in electricity demand and wind availability [28–31]. Also, in some works other features such as branches and generation constraints are explicitly included in the formulation such as presented in [32–34]. Other authors have made comparisons and analysis between this approach and conventional methods without these variables [35]. On the other hand, some works employs heuristic approaches including deterministic and stochastic methods (e.g Montecarlo simulation) to solve the optimal dispatching [36–41].

Several studies [42–45] have researched the integration of intermittent wind power using a probabilistic approach. In order to provide better tools for the construction of generation scenarios and stochastic dispatch models [46–48]. Consequently, optimal power flow has also been used with ESS in order to assess the power system operation flexibility [49], due to these units can absorb energy in case of excessive generation or low electricity prices, mitigating the uncertainty in the renewable sources. Also in this research topic, studies such [50, 51] have found other issues such as inclusion of ESS in distributed generation (DG) and RES with their respective modelling and sizing.

Other studies [11, 52–54] propose approaches in the economic dispatch using multi-period OPF due to specific challenges to the traditional OPF such as the modeling of charge/discharge of ESS, or a specific ESS technology featuring [55]. Other studies have included more variables in order to bring the problem closer to a more precise context such as [56, 57] using power losses constraints on the transmission branches to evaluate different generation scenarios. On the other hand, in [58] adds an environmental approach, modeling the social cost using variables such as emission generation in order to optimize the total production costs, using as little as possible the thermal generation, without neglecting the reliability in the system, all of this cases working under a DC approach.

2. DC-BASED OPTIMAL POWER FLOW WITH ESS

This section includes the notation and the mathematical formulation for the multiperiod DCOPF dispatching model including the ESS modeling. This model also includes thermal and wind power generation.

2.1. Notation

g	Thermal generation unit.
i, j	Network buses connected by transmission branches.
t	Time period (hours).
η_c, η_d	Charging/Discharging efficiency of the ESS units.
G	Number of thermal generation units.
L	Number of network branches.
T	Time period in the operating horizon, in this case 24 hour.
N	Number of network buses.
V_{WL}	Wind power waste value ($/MWh).
C_{ch}, C_{dch}	ESS Charging/Discharging marginal cost ($/MWh).
X_{ij}	Branch reactance connecting the i-bus to j. (p.u)
b_g	Fuel cost coefficient of thermal units ($).
P_g^{max}, P_g^{min}	Maximum/Minimum power generation thresholds of the thermal unit g (MW).
PL_{ij}^{max}	Maximum power flow boundaries of branch connecting the i-bus to j (MW).
P_{max}^{ch}, P_{min}^{ch}	Maximum/Minimum charge power limits for the ESS unit connected on the i-bus (MW).
P_{max}^{dch}, P_{min}^{dch}	Maximum/Minimum discharge power limits for the ESS connected on the i-bus (MW).
CS_{max}, CS_{min}	Maximum/Minimum energy stored (MWh).
$D_{i,t}$	Electric power load in the i-bus at time t.
Av_t^{wind}	Wind turbine availability on the i-bus at time t (MW).
C_t^{wind}	Wind turbine capacity connected on the i-bus (MW).
R_g^{up}, R_g^{down}	Ramp-up/down thresholds of thermal generation unit g (MW/h).
$PL_{ij,t}$	Active power flow from the i-bus to j-bus at time t (MW).
$P_{i,t}^{Gen}$	Active power generated by thermal unit g at time t (MW).
$P_{i,t}^{wind}$	Active power of wind turbine connected to i-bus at time t (MW).
$P_{i,t}^{wl}$	Curtailed power of wind turbine connected to the i-bus at time t (MW).
$\lambda_{i,t}$	Dual variable that denote Locational Marginal Price in the i-bus at time t ($/MWh).
F_{obj}	24-hour Total operating costs ($).
$\theta_{i,t}$	Voltage angle of the i-bus at time t (rad).
$CS_{i,t}$	Energy stored in the i-bus at time t (MWh).
$P_{i,t}^{ch}$,$P_{i,t}^{dch}$	Power Charged/discharged to/from ESS connected to the i-bus at time t (MW).

2.2. Formulation

The formulation is expressed as optimization problem to address a minimum total operating cost associated with producing electricity to meet the demand for a 24-hour period described by (1). In (2) indicates the total cost of energy production with g thermal units during an interval of time T. In (3) refers to the production costs associated with not taking full advantage of the source of wind generation available during this same interval of time. In (4) represents a condition that requires that the ESS are not charged and discharged simultaneously, this prevents the payment of an ESS for charging and discharging simultaneously [11, 29, 59], situation that cannot occur.

$$F_{obj} = C_G + W_L + C_{ESS} \quad (1)$$

$$C_G = \sum_{t=1}^{T}\sum_{g=1}^{G} b_g P_g^{Gen} \quad (2)$$

$$W_L = \sum_{t=1}^{T}\sum_{i=1}^{N} V_{WL} P_{i,t}^{wl} \quad (3)$$

$$C_{ESS} = \sum_{t=1}^{T}\sum_{i=1}^{N} (C_{dch} P_{i,t}^{dch} - C_{ch} P_{i,t}^{ch}) \quad (4)$$

The restrictions for the dispatching model are given by the power flow equations. This paper uses the DC approach to include power flow calculations. The power flow balance is given by (5). The power flowing on each line is given by (6). The power flow restrictions are given by the boundaries in the (7).

$$\sum_{g=1}^{G} P_{g,t}^{Gen} + P_{i,t}^{wind} - D_{i,t} - P_{i,t}^{ch} + P_{i,t}^{dch} = \sum_{j=1}^{L} PL_{ij,t} \quad (5)$$

$$PL_{ij,t} = \frac{1}{X_{ij}} (\theta_{i,t} - \theta_{j,t}) \quad (6)$$

$$-PL_{ij,t}^{max} \leq PL_{ij,t} \leq PL_{ij,t}^{max} \quad (7)$$

The dual variable associated to (5) correspond to the locational marginal price (LMP) of each bus hourly. On the other hand, the restrictions for thermal generation units are defined in (8), (9), and (10), where (8) corresponds to the operational range of thermal generators. On the other hand, (9) and (10) indicates the maximum up and down ramps limits that each of the thermal generators can perform from one hour to the next.

$$P_{g,t}^{min} \leq P_{g,t}^{Gen} \leq P_{g,t}^{max} \quad (8)$$

$$P_{g,t}^{Gen} - P_{g,t-1}^{Gen} \leq R_g^{up} \quad (9)$$

$$P_{g,t-1}^{Gen} - P_{g,t}^{Gen} \leq R_g^{down} \quad (10)$$

The energy level (i.e. State of charge) of ESS were defined per unit in the i-bus at time interval t, depends on the difference between the ESS charged and discharged power with their respective operating efficiencies, as defined in (11). The maximum and minimum limits of ESS charge/discharge, and ESS Capacity were defined in (12), (13) and (14) respectively.

$$CS_{i,t} - CS_{i,t-1} = \eta_c P_{i,t}^{ch} - \frac{P_{i,t}^{dch}}{\eta_d} \quad (11)$$

$$P_{i,min}^{ch} \leq P_{i,t}^{ch} \leq P_{i,max}^{ch} \quad (12)$$

$$P_{i,min}^{dch} \leq P_{i,t}^{dch} \leq P_{i,max}^{dch} \quad (13)$$

$$CS_{i,min} \leq CS_{i,t} \leq CS_{i,max} \quad (14)$$

The restrictions for wind generation (i.e. wind power loss) are defined in (15). The expression corresponds to the reduction of use of potentially available wind energy. In (16) describes the minimum and maximum power range that a wind generator can produce, considering placing and wind availability.

$$P_{i,t}^{wl} = Av_t^{wind} \cdot C_i^{wind} - P_{i,t}^{wind} \quad (15)$$

$$0 \leq P_{i,t}^{wind} \leq Av_t^{wind} \cdot C_i^{wind} \quad (16)$$

3. RESULT AND DISCUSSION

In order to test this approach to study a wide range of applications, initially, a small case and then a modified IEEE standard case are used to illustrate the ESS modelling in a multi-period dispatching and show their performance according to different operational situations. This section provides a comprehensive explanation of each case and the corresponding analysis to observe ESS performance during a 24-hour period.

All simulations were completed by a computer (PC) running Windows® with an Intel® Core I5+ 8300H processor @2.3 GHz with 12.00 GB RAM, using Gurobi® Solver (8.1.1) [60] under the JuMP 0.20.1 Julia platform [61].

3.1. Load curve description

The daily load curves used for the 5-bus (orange) and 24-bus (blue) power systems are plotted in Figure 1. The load curves present four (4) decreasing trend bands with its lowest point at hour 4 (i.e. 787.1 MW and 1950.6 MW respectively), and three (3) increasing trend bands with a load peak at hour 20 (i.e. 1150 MW and 2850 MW respectively).

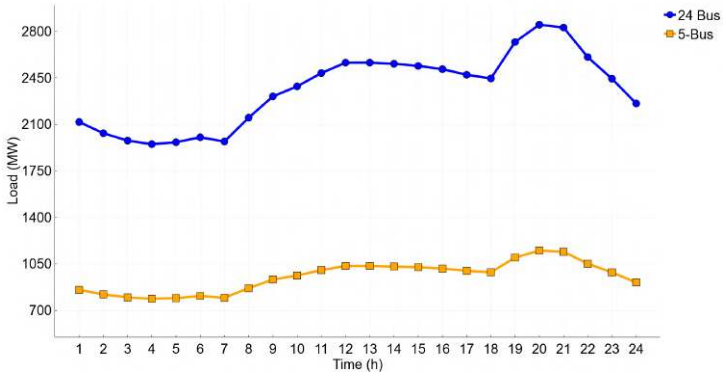

Figure 1. Load curve pattern for power systems testing

3.2. Wind availability profiles

Three (3) wind profiles are constructed to evaluate the ESS performance during the operation of both power systems considering wind power availability (i.e. low, moderate, and high) as shown in Figure 2. The simulation results of both power systems, such as the the thermal generators scheduling and the ESS performance as well as their respective analysis can be found in the following subsections.

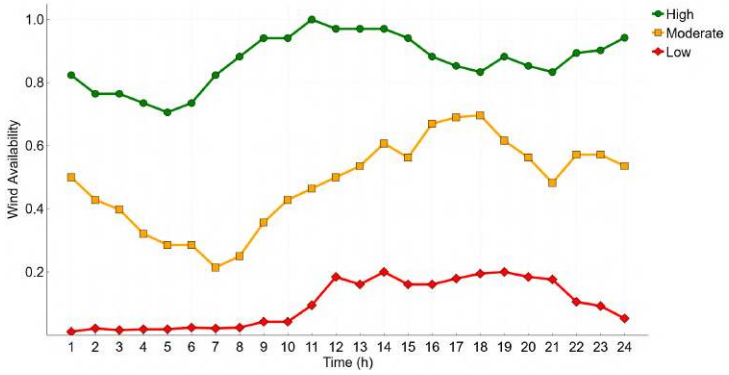

Figure 2. Wind availability profiles used for power systems testing

3.3. ESS performance in a 5-Bus system

3.3.1. Case description

The one-line diagram for a 5-Bus system is shown in Figure 3. This system includes thermal generation, wind generation and storage. The thermal unit parameters are listed in Table 1, modifying the information from [49]. The load is distributed in 4 buses.

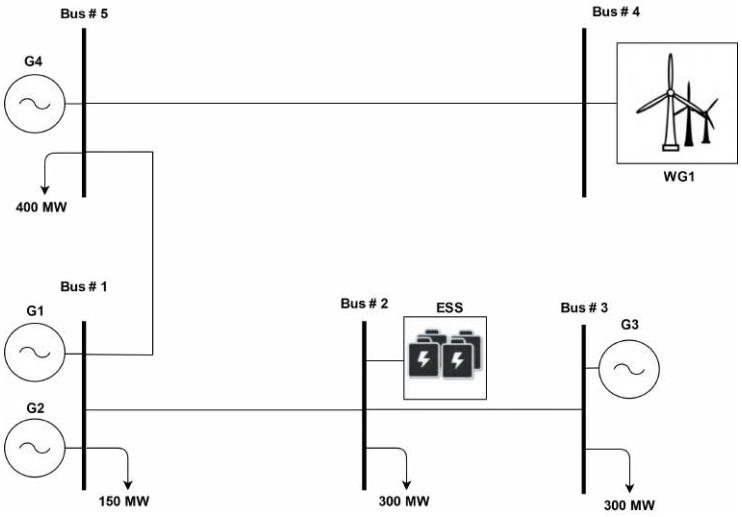

Figure 3. One-line diagram of modified 5-bus power system

Table 1. Thermal generation info for the 5-bus power system

Gen	Bus	P_g^{min}(MW)	P_g^{max} (MW)	Marginal Cost (MW)	R_g^{up} (MW/h)	R_g^{down} (MW/h)
1	1	0	140	17	20	20
2	1	0	170	18	25	25
3	3	0	360	20	30	30
4	5	0	490	21	35	35

Table 2 lists the network grid information such as reactance and rating in MVA (i.e power line constraints), all of them modified from [49].

Table 2. Branch info for the 5-bus test system

From	To	X_{ij} (p.u)	Rating (MVA)
1	2	0.0281	400
1	5	0.0064	400
2	3	0.0108	400
4	5	0.0297	240

The 5-bus test system includes a wind power plant connected to the bus 4. The wind power generation site and capacity is listed in Table 3. Also, this system includes an ESS connected in the bus 2. In other words, the ESS is not on the same bus as the wind power plant. The ESS parameters considered are ESS capacity, charging and discharging efficiency, and operating values. Such features are listed in Table 4.

Table 3. Wind power generation info for the 5-bus system

Gen	Bus	$C_{i,t}^{wind}$ (MW)
1	4	240

Table 4. ESS info for 5-bus system.

ESS	Bus	Capacity (MW)	η_c (%)	η_d (%)	$CS_{i,min}$ (%)	$CS_{i,max}$ (%)
1	2	50	90	90	10	90

3.3.2. Results

The simulations use the 5-bus power system with the parameters given before (i.e. load curve and wind profiles) to explore and evaluate different operational situations. Initially, the performance of the power system was evaluated according to gradual increases of the ESS capacity, starting from its base capacity (i.e. 25 MW steps, starting at 50 MW up to 200 MW). The analysis highlights changes in the thermal generation scheduling and ESS performance during the 24-hour period.

The ESS performance (i.e State of Charge (SoC)) during a 24-hour period is shown in Figure 4. Likewise, the ESS charging intervals occurs at hours 3 to 7, 16 to 18, and 23 to 24. A one ESS discharging interval occurs in the load peak value (hours 19 to 21). The ESS is charged in valley hours (low demand) and discharged at load peak hours (i.e. time shifting effect and transmission curtailment reduction) as expected. On the other hand, the ESS performance shows a gap when its capacity reaches 150 MWh and the wind availability improves (i.e. moderate and high availability). This finding is presented in hours where there is no charging or discharging behavior (i.e. hours 5 to 16).

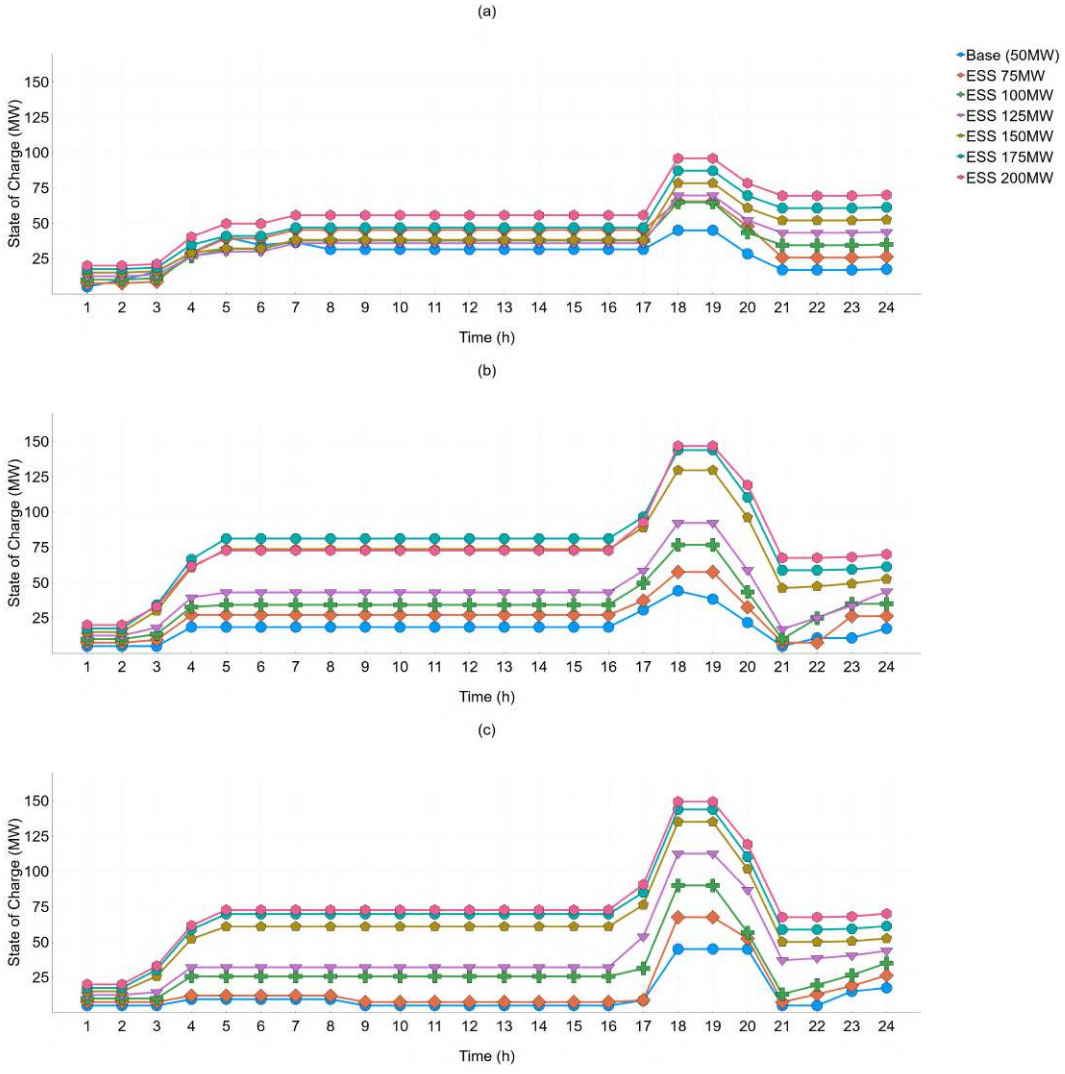

Figure 4. (a) Comparison of ESS performance between the low-wind availability, (b) the moderate wind availability, (c) and high-wind availability

The description of the ESS performance leads to the analysis that the of ESS installed capacity could be oversized due to wind availability. This could happen in low-wind availability due to wind turbines and

thermal units wouldn't have enough power to contribute meeting demand and charge the ESS at the same time, unless the wind availability increases. Therefore, two or more ESS with different capacities could have similar SoC values where the higher capacities are underutilized. Since it would not have complete charging cycles (e.g 200 MW and 175 MW ESS capacities in all wind patterns) thus decreasing its life cycle, and represents a smaller reduction in operating costs. This analysis shows that even in small power systems, features such as the ESS capacity must be analyzed technically and economically in a strict way.

On the other hand, the different thermal generation schedules according to the ESS capacity increases during a 24-hour period are shown in Figure 5. Similar performances to the proposed demand curve are presented especially in the low-availability wind pattern. Nonetheless, such performances moved away as wind availability increases (i.e. moderate and high availability patterns) as in the case of ESS performance. Furthermore, it can be appreciated differences in thermal scheduling between ESS capacities on valley hours (i.e hours 2 to 6, and hours 17 and 18) of the load curve for all wind patterns. Also, another difference between scheduling is presented at the peak of the load curve (i.e hours 20 and 21).

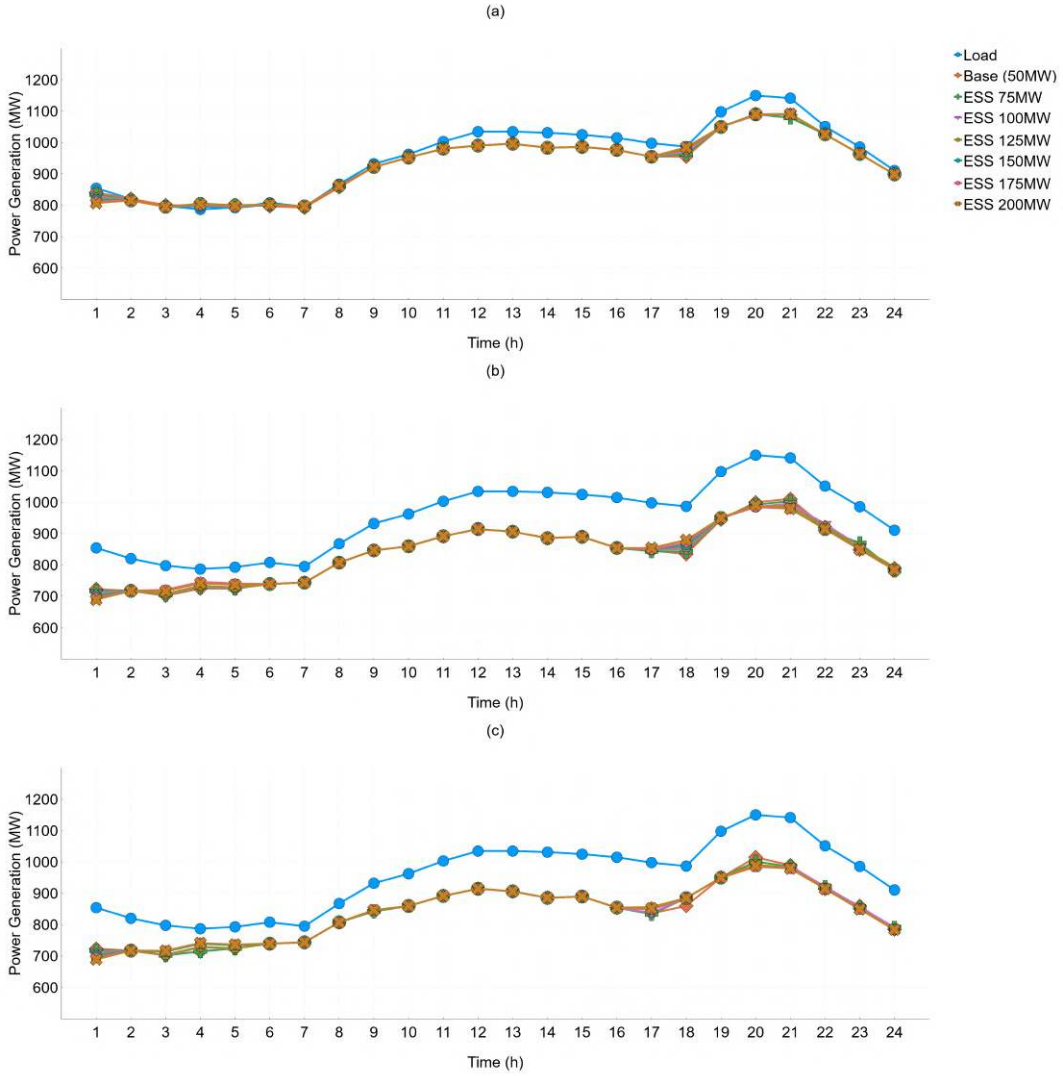

Figure 5. (a) Comparison of thermal scheduling between the low-wind availability, (b), the moderate wind availability, (c), and high-wind availability

Additionally, the thermal units dispatching under different wind availability patterns shows that wind availability determines the dispatching of thermal units. The proposed system has a limited generation portfolio

with a strong dependence on thermal units and low wind power participation. this factor explains the closeness between thermal scheduling and the load curve specially under low wind availability patterns and how similar behaviour is maintained regardless of wind availability. In the same way, the thermal unit scheduling between the highest proposed ESS capacities (e.g. 175 and 200 MW) are similar. This finding proved the misuse of ESS from a certain capacity and wind availability as mentioned above. Likewise, this issue represents a non-improvement of the power system performance as well as a negligible reduction of thermal generation compared with increases in the ESS capacity.

Moreover, The ESS performance seen from its SoC during a 24-hour period is shown in Figure 6. Unlike the previous scenario, It shows no differences for some of the proposed availability patterns. Since in low availability pattern, the ESS presents the same behavior regardless of the increase in marginal cost (i.e from 1.0 to 2.0 times). In all cases, charging and discharging patterns are presented depending on the respective wind pattern behavior. However, there is a consistent unloading pattern during peak hours (i.e. from hours 19 to 21). This represents the correct ESS modeling and operation since it delivered power during the load peak as expected.

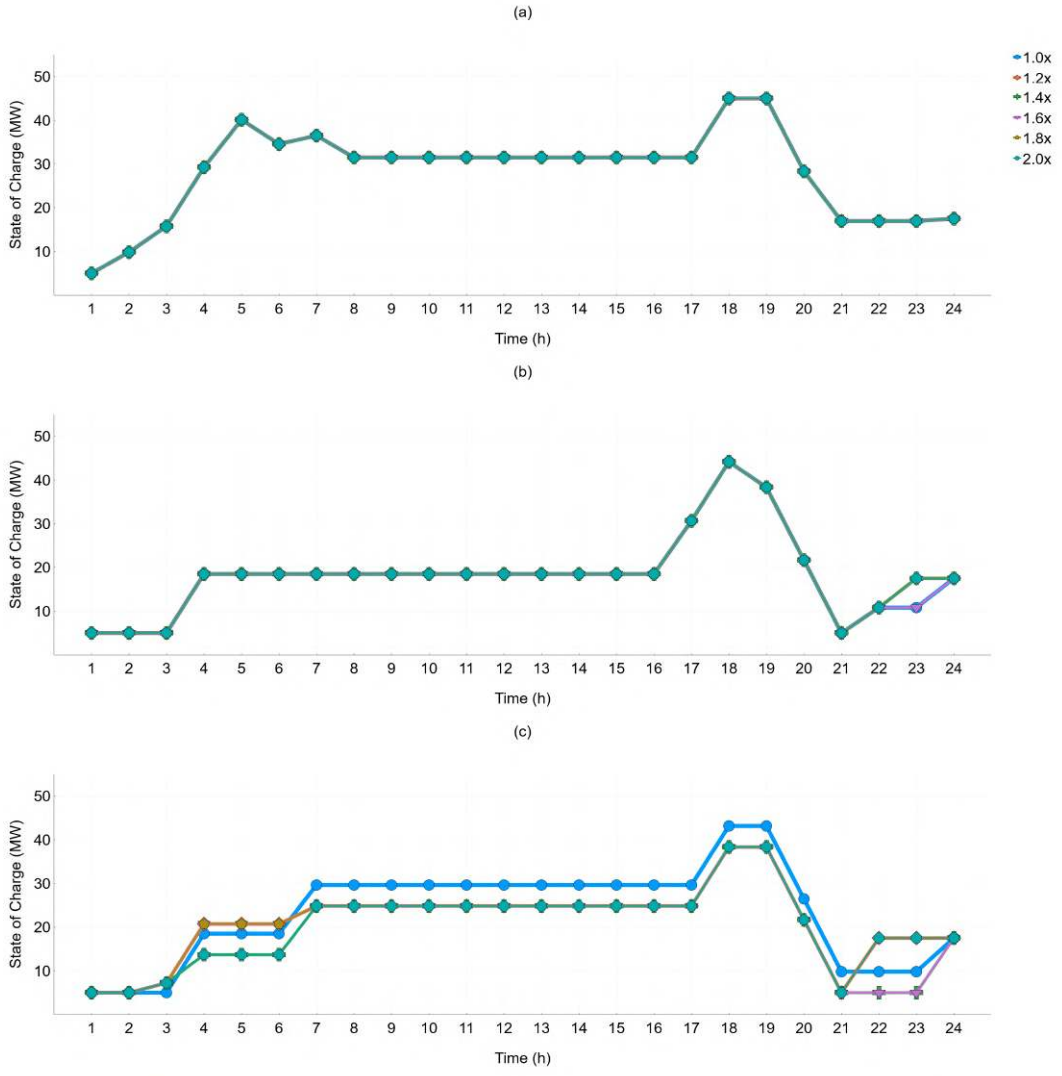

Figure 6. (a) Comparison of ESS performance with regard to the marginal cost increasing, between the low-wind availability, (b) the moderate wind availability, (c) and high-wind availability

Also, the ESS performance shows a direct influence by wind availability due to the fact that the ESS

finds some operation flexibility by increasing wind availability. Thus, in low wind availability the storage system in most of the time tends to charge until load peak hours regardless of the marginal cost of the thermal units, while in moderate or high wind availability depending on the marginal cost different behaviors can be presented (that is to say power amounts and charge or discharge decisions) of the ESS. Nonetheless, although different performances according to the marginal fuel cost are presented, in general terms the ESS performed in a similar way.

In other matters, the thermal units dispatch according to wind availability and compared to the load curve is shown in Figure 7. It shows similar behaviors between the thermal scheduling and the load curve for all wind availability profiles, in some cases (i.e. hours 1 to 7 in low-wind availability) the load curve and the thermal units dispatch have matched. Thus, the thermal unit dispatch also shows few changes by increasing the marginal cost to the proposed value. These changes were presented when load falls (i.e. hours 3 to 7 and hours 19 to 24) and exist high wind availability, as shown in c). For all other wind availability patterns, the same thermal units power dispatch was presented.

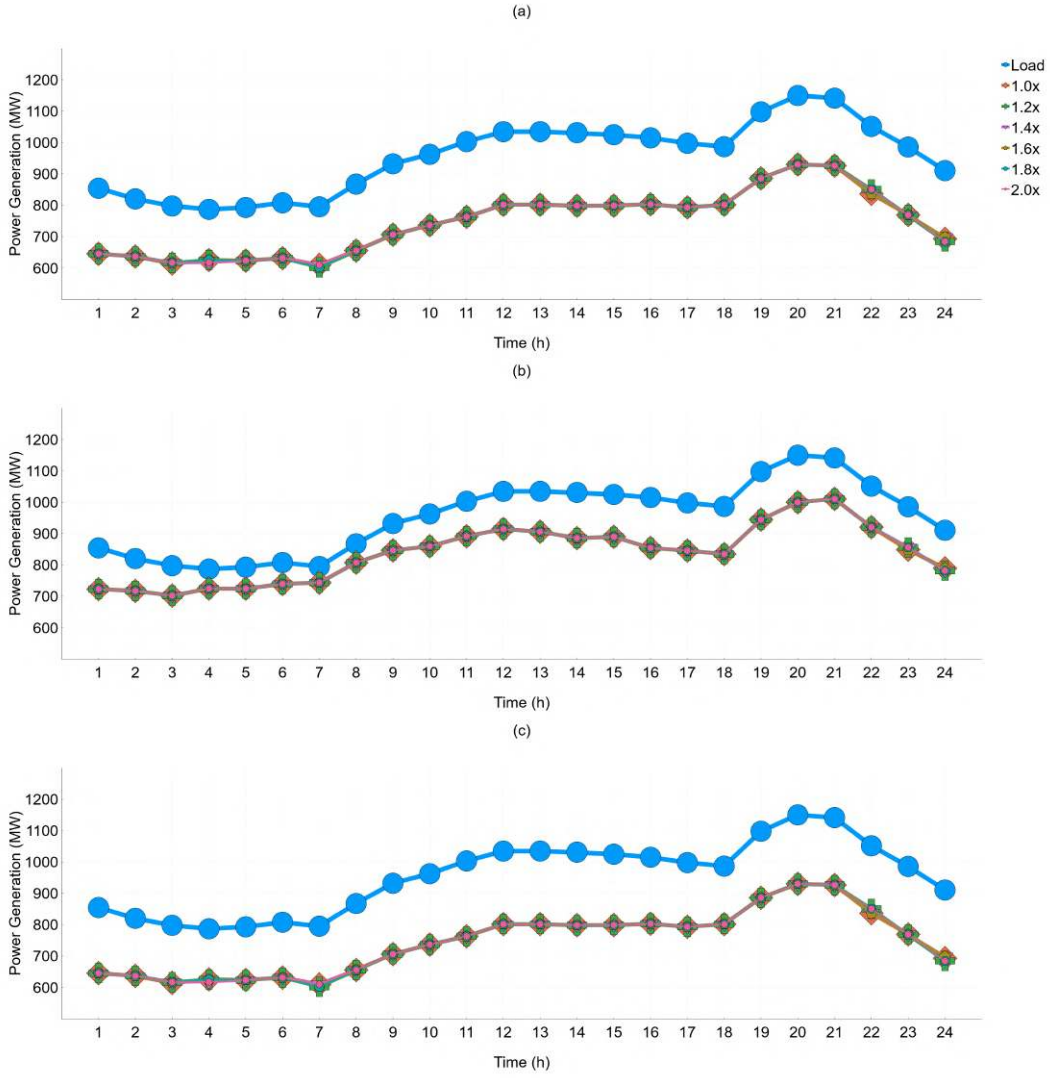

Figure 7. (a) Comparison of thermal unit scheduling with regard to the marginal cost increasing, between the low-wind availability, (b) the moderate wind availability, (c) and high-wind availability

Furthermore, the the wind availability effect on the power system is evident since the difference between load and thermal units power is greater (i.e. differences between low, moderate and high wind availability

for all marginal cost increases). In other words, since the generation portfolio of this power system is mostly thermal the dispatched amounts were similar due to the non-existence of meaningful alternative resources to meet demand. Nevertheless, the wind power and ESS would represent a feasible option for mitigating the increased costs of producing with thermal units as proposed.

3.4. ESS performance in the IEEE 24-Bus System

3.4.1. Case description

The one-line diagram for a modified IEEE 24-bus power system is shown in Figure 8. As above, this system includes thermal generation, wind generation and storage. The thermal unit features are listed in Table 5, modifying the information from [49]. The load is distributed in 16 buses.

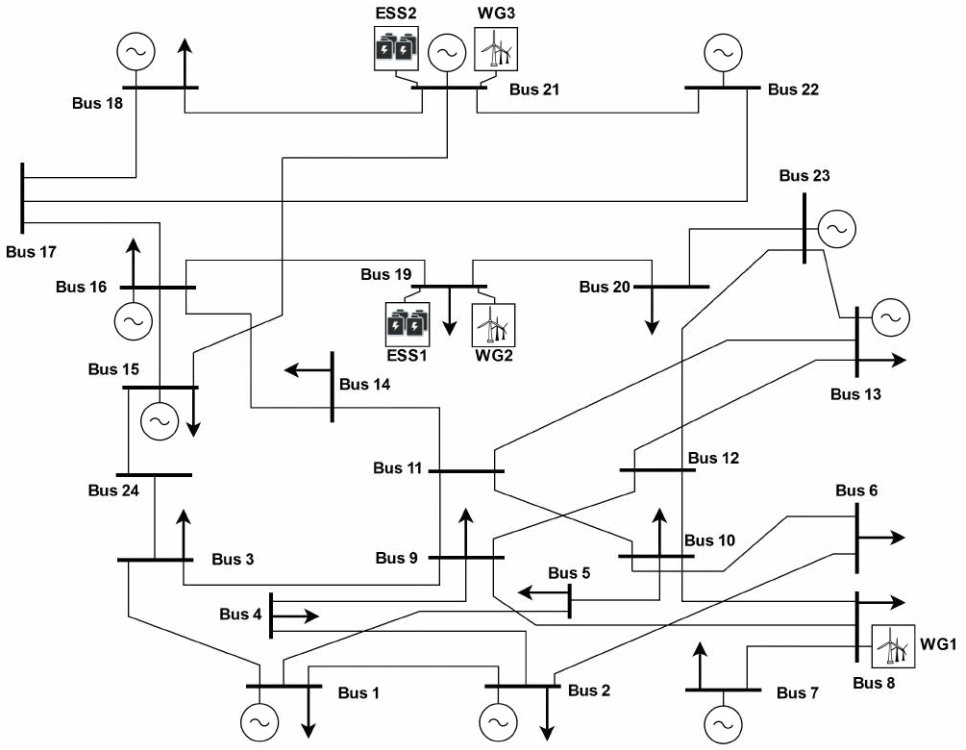

Figure 8. One-line diagram: 24-bus power system

Table 5. Thermal generation data for the 24-bus test system

Gen	Bus	P_g^{min}(MW)	P_g^{max} (MW)	Marginal Cost (MW)	R_g^{up} (MW/h)	R_g^{down} (MW/h)
1	18	100	400	5.47	47	47
2	21	100	400	5.49	47	47
3	1	30.4	152	13.32	14	14
4	2	30.4	152	13.32	14	14
5	15	54.25	155	16	21	21
6	16	54.25	155	10.52	21	21
7	23	108.5	310	10.52	21	21
8	23	140	350	10.89	28	28
9	7	75	350	20.7	49	49
10	13	206.85	591	20.93	21	21
11	15	12	60	26.11	7	7
12	22	0	300	0	35	35

Table 6 lists the network grid information such as reactance, power line constraints and interconnections, all of them directly from [49].

Table 6. Branch data for the 24-bus test system

From	To	X_{ij} (p.u)	Rating (MVA)	From	To	X_{ij} (p.u)	Rating (MVA)
1	2	0.0281	400	18	2	0.0281	400
2	5	0.0064	400	19	2	0.0281	400
3	3	0.0108	400	20	2	0.0281	400
4	5	0.0297	240	21	2	0.0281	400
5	2	0.0281	400	22	2	0.0281	400
6	5	0.0064	400	23	2	0.0281	400
7	3	0.0108	400	24	2	0.0281	400
8	5	0.0297	240	25	2	0.0281	400
9	2	0.0281	400	26	2	0.0281	400
10	5	0.0064	400	27	2	0.0281	400
11	3	0.0108	400	28	2	0.0281	400
12	5	0.0297	240	29	2	0.0281	400
13	2	0.0281	400	30	2	0.0281	400
14	5	0.0064	400	31	2	0.0281	400
15	3	0.0108	400	32	2	0.0281	400
16	5	0.0297	240	33	2	0.0281	400
17	5	0.0297	240	34	2	0.0281	400

This power system includes three wind power plants connected to buses 8, 19 and 21. The different sizes of these wind plants are shown in Table 7. Likewise, the system includes two ESS connected to buses 19 and 21 respectively (i.e. the ESS are in buses where wind power plants are located, unlike the case above), where their features (i.e. charging/discharging efficiency, capacity, among others) are listed in Table 8.

Table 7. Wind power generation data for the 24-bus test system

Gen	Bus	$C_{i,t}^{wind}$ (MW)
1	8	200
2	19	150
3	21	100

Table 8. Wind power generation data for the 24-bus test system

ESS	Bus	Capacity (MW)	η_c (%)	η_d (%)	$CS_{i,min}$ (%)	$CS_{i,max}$ (%)
1	19	200	90	90	10	90
2	21	100	90	90	10	90

3.4.2. Results

The simulations use the 24-bus power system with the parameters (load curve and wind profiles) given above. The analysis highlights changes in thermal units scheduling and ESS performance during the 24-hour period as above.

The ESS performance during a 24-hour period is shown in Figure 9. It shows different performances for all wind patterns tested. In other words, the initial charging behavior for each wind availability pattern occur at different times (i.e. hours 4 to 7 in low availability, hours 1 to 8 in moderate availability, and hours 6 to 8 in high availability). However, the discharging behavior that occurs at the peak area of the purposed load curve (hours 18 to 21) remains the same. Likewise, the increase in the capacity of the ESS has no effect on the general ESS performance. Moreover, the proper performance of the mathematical modeling of the ESS also was verified.

Likewise, the ESS capacity installed in this power system presents an adequate capacity unlike the 5-bus case. This is due to the fact that regardless of the purposed wind availability profile, the ESS provides energy at the time when the load peak occurs (i.e. an average of 150 MW of the 2850 MW of load). Another fact to support that statement is the ESS capacity presented in each increment and wind availability pattern is totally used (minimum and maximum allowed ESS capacities) avoiding misusing. In fact, this result motivates to increase the ESS base capacity to achieve lower total operating costs.

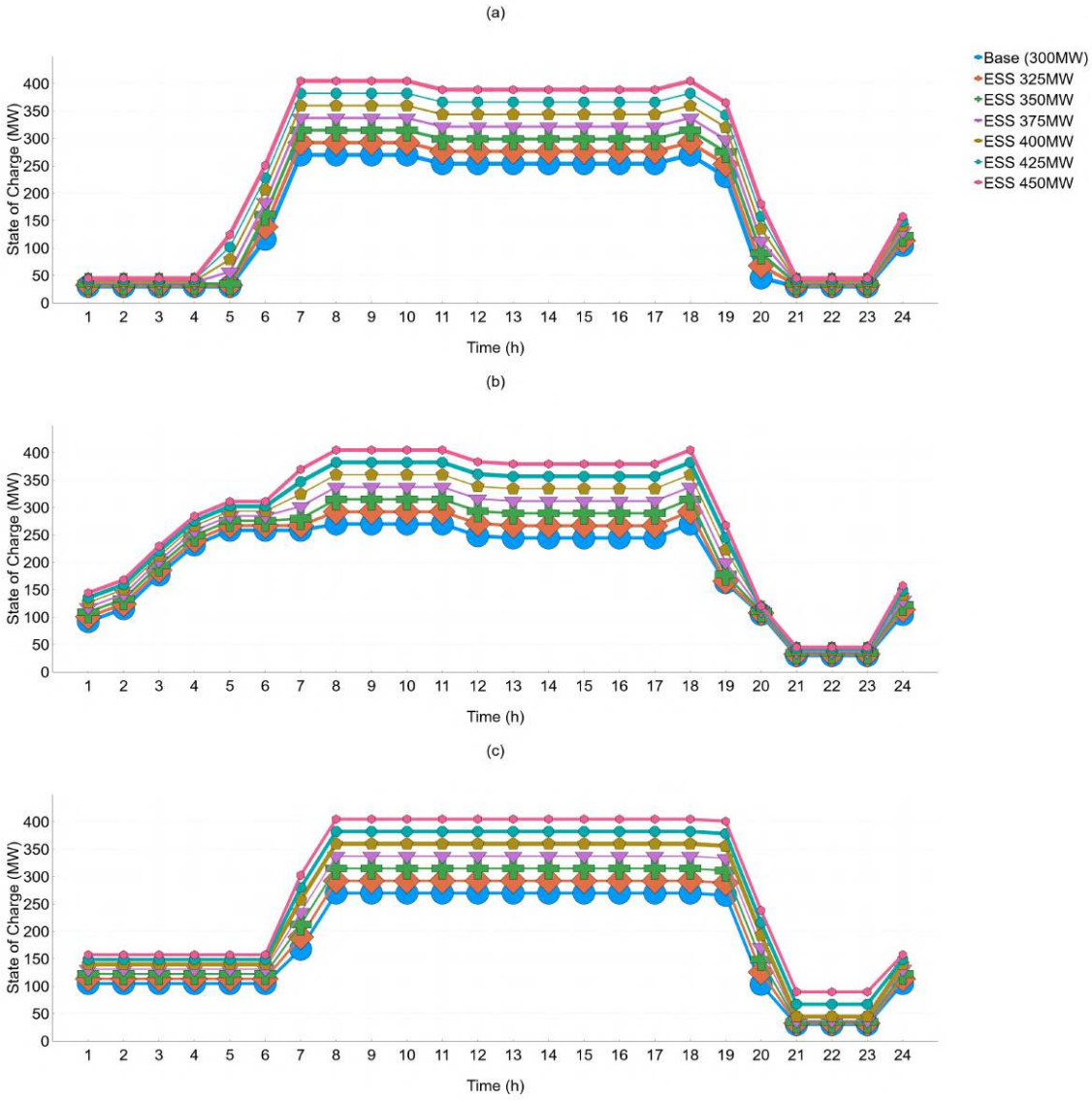

Figure 9. (a) Comparison of ESS performance in 24-bus system between the low-wind availability, (b) the moderate wind availability,(c) and high-wind availability

On the other hand, the different thermal generation units schedules according to ESS capacity increases during the 24-hour period for this system are shown in the Figure 10. Similar performances to the proposed load curve are presented especially in the low-availability wind pattern (except for hours 5 to 7, due to excess electrical energy of this technology subsequently stored in the ESS). Also it can be appreciated differences in thermal scheduling between ESS capacities on valley hours (i.e hours 2 to 6, and hours 17 and 18) of the load curve for all wind patterns. Likewise, another difference between scheduling is presented at the peak of the load curve (i.e hours 20 and 21).

Additionally, the thermal units dispatching under different wind availability patterns shows that wind availability strongly determines the thermal units dispatch. As well as the 5-bus system, this system presents a portfolio with a predominance of electricity produced by thermal units and lower wind power participation. This situation is highlighted in the system especially in the low wind availability, because the thermal units must produce above the load to satisfy the programming of the whole 24-hour period (i.e. hours 5 to 7). Fortunately, since the power system has ESS with adequate capacity, it can store this amount of excess energy to deliver when required.

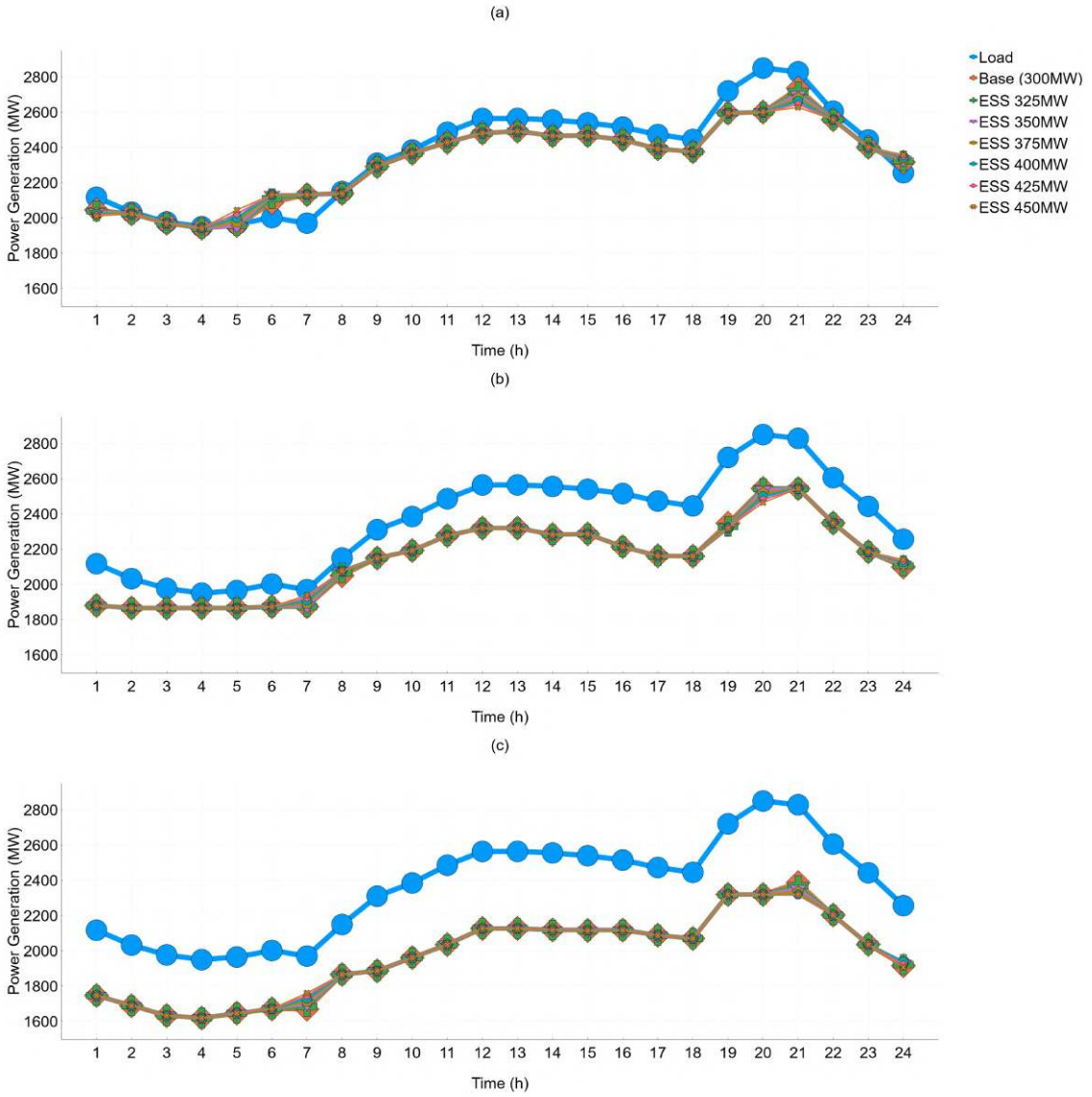

Figure 10. (a) Comparison of thermal scheduling in 24-bus system between the low-wind availability, (b) the moderate wind availability, (c) and high-wind availability

Like the previous case, the power system performance also was evaluated under the effect of gradually increasing the marginal cost per MW of thermal units until doubling its value (i.e. 0.2 times steps, from 1.0 to 2.0 times). This analysis explores this operational situation with more expensive thermal generation due to increment in the cost of fuel such as coal or gas, and how this affects the dispatching performance. This analysis highlights changes in the 24-bus system thermal generation scheduling and ESS performance during the 24-hour period.

The ESS performance seen from its SoC during a 24-hour period is shown in Figure 11. It shows no differences for the proposed wind availability profiles. Due to the ESS presents the same behavior regardless of the increase in marginal cost (i.e from 1.0 to 2.0 times). In all cases, charging patterns appear depending on the respective wind pattern behavior. However, again there is a consistent discharging pattern during peak hours (i.e. hours 19 to 21) and different charging patterns at the beginning of the analysis period (i.e. hours 5 to 7 in low availability, 2 to 5 in moderate availability, and 6 to 7 in high availability).

Furthermore, It also shows an influence by wind availability due to the ESS finds some operation flexibility by increasing wind availability, delivering the stored energy when it is really needed (i.e. load peak

hours). This fact is evidenced by the decrease in the amount of charging and discharging interactions when the highest wind availability occurs. However, the marginal cost increase has no impact on the performance of the ESS and does not prevent the use of all the capacity that this device allows.

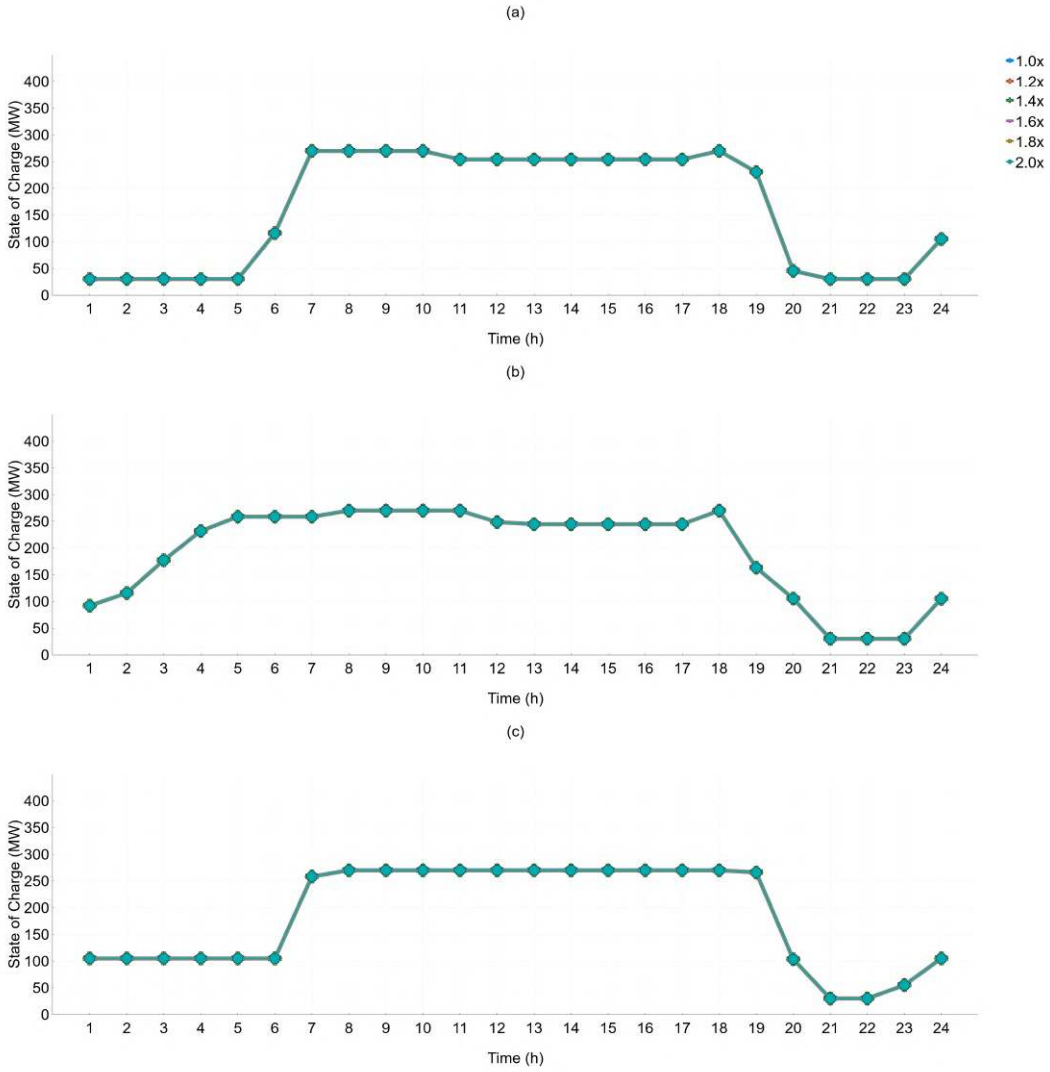

Figure 11. (a) Comparison of ESS performance with regard to the marginal cost increasing for a 24-bus system, between the low-wind availability, (b), the moderate wind availability, (c) and high-wind availability

The thermal units dispatch according to wind availability for the 24-bus system and compared to the load curve is shown in Figure 12. It shows similar performances between the thermal scheduling and the proposed load curve for all wind pattern. Again the thermal units dispatch exceeds the load to complete the 24-hour scheduling period (i.e. hours 6 to 7 in low-wind availability graph). Also, the thermal units dispatch is unchanged when increasing the marginal cost to the proposed value for all wind availability patterns. The difference between the load curve and thermal unit scheduling for all cases and wind patterns corresponds to the variable wind power participation and the charging/discharging interactions carried out by the ESS included in the system.

Likewise, the impact of wind availability in this power system is evident since the difference between load and thermal units power is greater. The generation portfolio of this power system is mostly thermal where the dispatched amounts were similar due to the non-existence of meaningful amount of alternative resources power to meet demand. This fact suggests a possible expansion of the total ESS capacity in this system, either

by increasing the existing ones or by placing new ones in other buses, due to the reduction of operational costs and thermal unit dependence that these devices represent as shown in the previous scenario. However, the location and capacity of these systems must be optimal to achieve this goal. This consideration involves solving a new optimization problem with that approach.

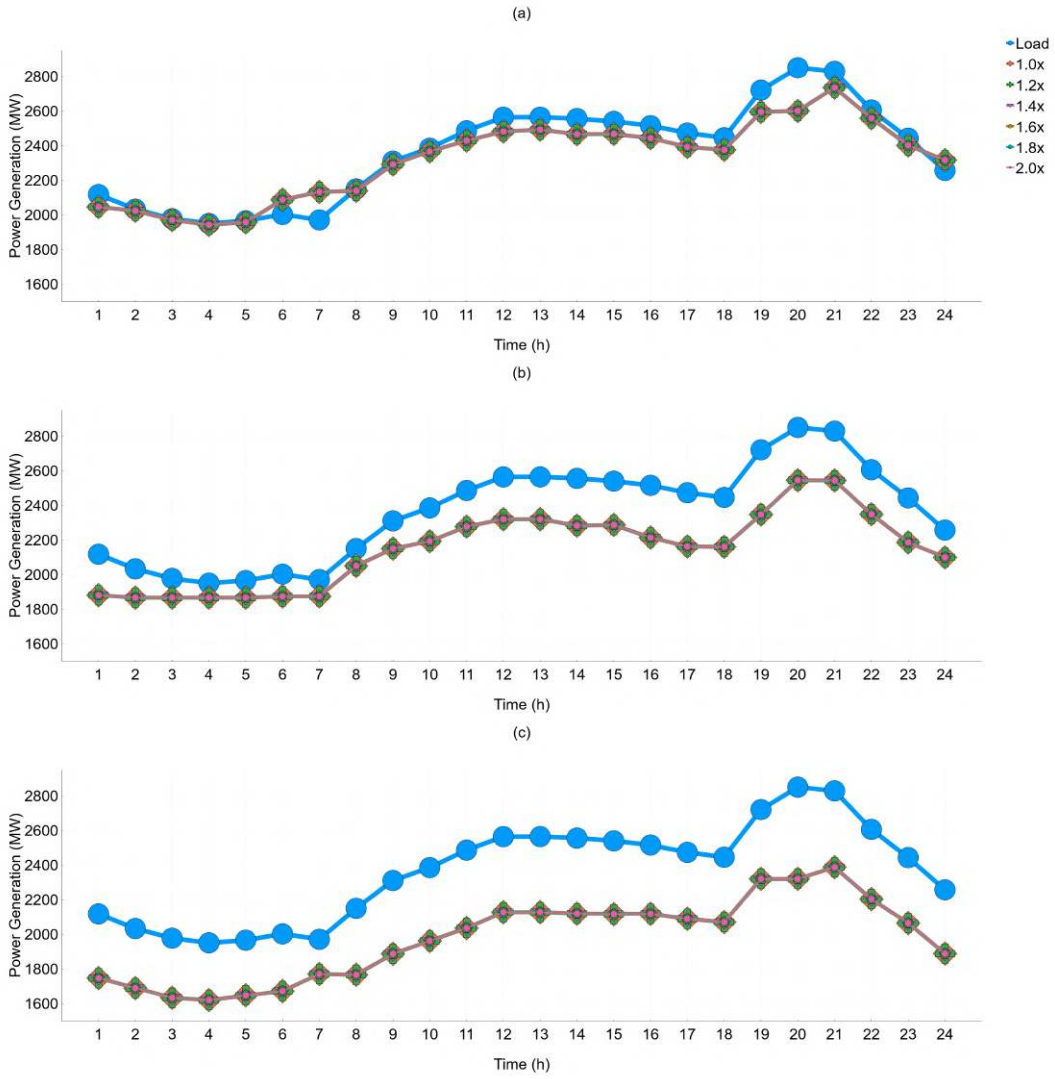

Figure 12. (a) Comparison of thermal scheduling with regard to the marginal cost increasing for a 24-bus system, between the low-wind availability, (b) the moderate wind availability, (c) and high-wind availability

4. CONCLUSION

In this article, a detailed multi-period DCOPF model for a 5-bus and a 24-bus power system was presented that includes renewable power (i.e wind power) and energy storage systems (ESS) under different operational scenarios for a 24-hour period. It has been shown that the mathematical modeling presented for the ESS charging and discharging behavior, corresponds to a valid approach of these elements for a planning process since it satisfies the dual features of this type of devices.

It was observed the great incidence of the wind availability for the proposed power system since it affects the ESS participation in load meeting, and thermal units dispatch even if the marginal cost is increased. It is due to the limited generation portfolio that is mostly thermal, being more susceptible to these changes. However, this feature causes the same thermal power to be dispatched even through marginal costs increase for

both systems, since both systems does not have meaningful alternative resources.

Moreover, when increasing the capacity of the ESS, different situations arose for the systems used. In the 5-bus system, above a certain ESS capacity, the system did not improve its performance or significantly reduce its operating cost. Consequently, an investment in ESS with such capacities would not be fully exploited, which could represent economic losses and higher cost for users. On the other hand, for the 24-bus system all the proposed increases in ESS capacity represented significant savings and improved system performance. Thus, the existence of an efficient use of the ESS was verified from all wind availability patterns and capacities tested. This is because all proposed ESS capacities are fully used. Thus, an investment in increasing ESS capacity from base capacity to target value (from 300 MW to 450 MW) represents meaningful operational cost savings as well as lower costs for users.

ACKNOWLEDGEMENT

The authors would like to thank the support of the Universidad Autónoma de Occidente in Cali, Colombia.

REFERENCES

[1] U. S. DOE, "Staff report to the secretary on electricity markets and reliability," *U.S. Department of Energy*, 2017.

[2] O. Ellabban, H. Abu-Rub, and F. Blaabjerg, "Renewable energy resources: Current status, future prospects and their enabling technology," *Renewable and Sustainable Energy Reviews*, vol. 39, pp. 748-764, 2014.

[3] L. E. Jones, "Renewable energy integration: practical management of variability, uncertainty, and flexibility in power grids," *Academic Press*, 2017.

[4] A. Foley and I. D. Lobera, "Impacts of compressed air energy storage plant on an electricity market with a large renewable energy portfolio," *Energy*, vol. 57, pp. 85-94, 2013.

[5] A. Foley and A. G. Olabi, "Renewable energy technology developments, trends and policy implications that can underpin the drive for global climate change," *Renewable and Sustainable Energy Reviews*, vol. 68, 2017.

[6] I. E. Agency, Renewables Information 2019. OECD Publishing, 2019. [Online]. Available: https://www.oecd-ilibrary.org/content/publication/fa89fd56-en

[7] J. M. Morales, A. J. Conejo, and J. Perez-Ruiz, "Short-term trading for a wind power producer," *IEEE Transactions on Power Systems*, vol. 25, no. 1, pp. 554-564, 2010.

[8] S. S. Sakthi, R. Santhi, N. M. Krishnan, S. Ganesan, and S. Subramanian, "Wind integrated thermal unit commitment solution using grey wolf optimizer," *International Journal of Electrical and Computer Engineering (IJECE)*, vol. 7, no. 5, pp. 2309-2320, 2017.

[9] K. Rabyi and H. Mahmoudi, "Energy storage of dfig based wind farm using d-statcom," *International Journal of Electrical and Computer Engineering (IJECE)*, vol. 9, no. 2, pp. 761-770 , 2019.

[10] A. Abdulla and T. Jiang, "Impact of compressed air energy storage system into diesel power plant with wind power penetration," *International Journal of Electrical and Computer Engineering (IJECE)*, vol. 9, no. 3, pp. 1553-1560, 2019.

[11] N. T. A. Nguyen, "Optimal planning of energy storage systems considering uncertainty," *Ph.D. dissertation, Politecnico di Milano*, 2016.

[12] F. Nadeem, et al., "Comparative review of energy storage systems, their roles, and impacts on future power systems," *IEEE Access*, vol. 7, pp. 4555–4585, 2018.

[13] X. Yu, X. Dong, S. Pang, L. Zhou, and H. Zang, "Energy storage sizing optimization and sensitivity analysis based on wind power forecast error compensation," *Energies*, vol. 12, no. 24, 2019.

[14] J. Rugolo and M. J. Aziz, "Electricity storage for intermittent renewable sources," *Energy and Environmental Science*, vol. 5, no. 5, pp. 7151-7160, 2012.

[15] N. Chowdhury, F. Pilo, and G. Pisano, "Optimal energy storage system positioning and sizing with robust optimization," *Energies*, vol. 13, no. 3, p. 512, 2020.

[16] C. K. Das, O. Bass, G. Kothapalli, T. S. Mahmoud, and D. Habibi, "Overview of energy storage systems in distribution networks: Placement, sizing, operation, and power quality," *Renewable and Sustainable Energy Reviews*, vol. 91, pp. 1205-1230, 2018.

[17] R. Moreno-Chuquen and J. Obando-Ceron, "Network topological notions for power systems security assessment," *International Review of Electrical Engineering (IREE)*, vol. 13, no. 3, pp. 237-258, 2018.
[18] R. Moreno-Chuquen and O. Florez-Cediel, "Online dynamic assessment of system stability in power systems using the unscented kalman filter," *International Review of Electrical Engineering (IREE)*, vol. 14, no. 6, 2019.
[19] H. R. Chamorro, et al., "Non-synchronous generation impact on power systems coherency," *IET Generation, Transmission and Distribution*, vol. 10, no. 10, pp. 2443-2453, 2016.
[20] U. S. DOE, "Solving challenges in energy storage," *U.S. Department of Energy*, 2018.
[21] A. Conejo and L. Baringo, "Power System Operations," *Springer*, 2018.
[22] H. Chamorro, M. Ghandhari, and R. Eriksson, "Wind power impact on power system frequency response," *North American Power Symposium (NAPS)*, pp. 1-6, 2013.
[23] Z. Li, Y. Cao, L. V. Dai, X. Yang, T. T. Nguyen et al., "Optimal power flow for transmission power networks using a novel metaheuristic algorithm," *Energies*, vol. 12, no. 22, 2019.
[24] A. Gabash and P. Li, "Active-reactive optimal power flow in distribution networks with embedded generation and battery storage," *IEEE Transactions on Power Systems*, vol. 27, no. 4, pp. 2026-2035, 2012.
[25] L. Ran, L. Zhengyu, and C. Zhen, "Economic dispatch of off-grid photovoltaic generation system with hybrid energy storage," *2nd IEEE Conference on Energy Internet and Energy System Integration (EI2)*, pp. 1-6, 2018.
[26] L. Zhou, Y. Huang, K. Guo, and Y. Feng, "A survey of energy storage technology for micro grid," *Power System Protection and Control*, vol. 39, no. 7, pp. 147-152, 2011.
[27] I. Yahyaoui, "Advances in Renewable Energies and Power Technologies: Volume 1: Solar and Wind Energies," *Elsevier*, 2018.
[28] R. A. Jabr, "Adjustable robust OPF with renewable energy sources," *IEEE Transactions on Power Systems*, vol. 28, no. 4, pp. 4742-4751, 2013.
[29] A. Castillo and D. F. Gayme, "Profit maximizing storage allocation in power grids," *52nd IEEE Conference on Decision and Control*, pp. 429-435, 2013.
[30] T. Geetha and V. Jayashankar, "Generation dispatch with storage and renewables under availability based tariff," *TENCON 2008-2008 IEEE Region 10 Conference*, pp. 1-6, 2008.
[31] A. Castillo and D. F. Gayme, "Evaluating the effects of real power losses in optimal power flow-based storage integration," *IEEE Transactions on Control of Network Systems*, vol. 5, no. 3, pp. 1132-1145, 2018.
[32] H. Sharifzadeh, N. Amjady, and H. Zareipour, "Multi-period stochastic security-constrained opf considering the uncertainty sources of wind power, load demand and equipment unavailability," *Electric Power Systems Research*, vol. 146, pp. 33-42, 2017.
[33] C. Boonchuay, K. Tomsovic, F. Li, and W. Ongsakul, "Robust optimization-based DC optimal power flow for managing wind generation uncertainty," *AIP Conference Proceedings*, vol. 1499. pp. 31-35, 2012.
[34] J. Obando-Ceron and R. Moreno-Chuquen, "Impacts of demand response under wind power uncertainty in network-constrained electricity markets," *IEEE ANDESCON*, pp. 1-5, 2018.
[35] R. Azami, M. Sadegh Javadi, and G. Hematipour, "Economic load dispatch and DC-optimal power flow problem-PSO versus LR," *International Journal of Multidisciplinary Sciences and Engineering*, vol. 2, no. 9, pp. 8-13, 2011.
[36] K. Seong-Cheol and S. R. Salkuti, "Optimal power flow based congestion management using enhanced genetic algorithms," *International Journal of Electrical and Computer Engineering (IJECE)*, vol. 9, no. 2, pp. 875-883, 2019.
[37] J. Lujano-Rojas, G. Osorio, J. Matias, and J. Catal-ao, "A heuristic methodology to economic dispatch problem incorporating renewable power forecasting error and system reliability," *Renewable Energy*, vol. 87, pp. 731-743, 2016.
[38] J. S. Obando, G. Gonzalez, and R. Moreno, "Quantification of operating reserves with high penetration of wind power considering extreme values," *International Journal of Electrical and Computer Engineering*, vol. 10, no. 2, pp. 1693-1700, 2020.
[39] R. Subramanian, K. Thanushkodi, and A. Prakash, "An efficient meta heuristic algorithm to solve economic load dispatch problems," *Iranian Journal of Electrical and Electronic Engineering*, vol. 9, no. 4, pp. 246-252, 2013.
[40] H. Sadeghian and M. Ardehali, "A novel approach for optimal economic dispatch scheduling of integrated

combined heat and power systems for maximum economic profit and minimum environmental emissions based on benders decomposition," *Energy*, vol. 102, pp. 1-23, 2016.
[41] E. Mojica-Nava, S. Rivera, and N. Quijano, "Game-theoretic dispatch control in microgrids considering network losses and renewable distributed energy resources integration," *IET Generation, Transmission and Distribution*, vol. 11, no. 6, pp. 1583–1590, 2017.
[42] R. Jabr and B. Pal, "Intermittent wind generation in optimal power flow dispatching," *IET Generation, Transmission and Distribution*, vol. 3, pp. 66-74, 2009.
[43] H. Zhang and P. Li, "Probabilistic analysis for optimal power flow under uncertainty," *IET Generation, Transmission and Distribution*, vol. 4, pp. 553-561, 2010.
[44] R. Entriken, A. Tuohy, and D. Brooks, "Stochastic optimal power flow in systems with wind power," *2011 IEEE Power and Energy Society General Meeting*, pp. 1-5, 2011.
[45] C. Saunders, "Point estimate method addressing correlated wind power for probabilistic optimal power flow," *IEEE Transactions on, Power Systems*, vol. 29, pp. 1045-1054, 2014.
[46] A. Papavasiliou and S. Oren, "Multi-area stochastic unit commitment for high wind penetration in a transmission constrained network," *Operations Research*, vol. 61, 2011.
[47] J. Obando-Ceron and R. Moreno-Chuquen, "Quantification of operating reserves with wind power in day-ahead dispatching," *IEEE ANDESCON*, pp. 1-5, 2018.
[48] R. Moreno, J. Obando, and G. Gonzalez, "An integrated opf dispatching model with wind power and demand response for day-ahead markets," *International Journal of Electrical and Computer Engineering (IJECE)*, vol. 9, no. 4, pp. 2794-2802, 2019.
[49] A. Soroudi, "Power System Optimization Modeling in GAMS," *Springer*, 2017.
[50] M. Asaduz-Zaman, M. H. Rahaman, M. S. Reza, and M. M. Islam, "Coordinated control of interconnected microgrid and energy storage system," *International Journal of Electrical and Computer Engineering (IJECE)*, vol. 8, no. 6, pp. 4781-4789, 2018.
[51] B. Banhthasit, C. Jamroen, and S. Dechanupaprittha, "Optimal generation scheduling of power system for maximum renewable energy harvesting and power losses minimization," *International Journal of Electrical and Computer Engineering (IJECE)*, vol. 8, no. 4, pp. 1954-1966, 2018.
[52] R. Jabr, S. Karaki, and J. Korbane, "Robust multi-period opf with storage and renewables," *IEEE Transactions on Power Systems*, vol. 30, pp. 2790-2799, 2015.
[53] Z. Wang, J. Zhong, D. Chen, Y. Lu, and K. Men, "A multi-period optimal power flow model including battery energy storage," *IEEE Power and Energy Society General Meeting*, pp. 1-5, 2003.
[54] Y. Levron, J. M. Guerrero, and Y. Beck, "Optimal power flow in microgrids with energy storage," *IEEE Transactions on Power Systems*, vol. 28, no. 3, pp. 3226–3234, 2013.
[55] A. Gonzalez-Castellanos, D. Pozo, and A. Bischi, "Detailed li-ion battery characterization model for economic operation," *International Journal of Electrical Power and Energy Systems*, vol. 116, 2020.
[56] B. Eldridge, R. O'Neill, and A. Castillo, "An improved method for the dcopf with losses," *IEEE Transactions on Power Systems*, vol. 33, no. 4, pp. 3779-3788, 2018.
[57] V. Hinojosa and F. Gonzalez-Longatt, "Preventive security-constrained DCOPF formulation using power transmission distribution factors and line outage distribution factors," *Energies*, vol. 11, 2018.
[58] P. Maghouli, A. Soroudi, and A. Keane, "Robust computational framework for mid-term technoeconomical assessment of energy storage," *IET Generation Transmission and Distribution*, 2015.
[59] B.-C. Jeong, D.-H. Shin, J.-B. Im, J.-Y. Park, and Y.-J. Kim, "Implementation of optimal two-stage scheduling of energy storage system based on big-data-driven forecasting—an actual case study in a campus microgrid," *Energies*, vol. 12, no. 6, 2019.
[60] Gurobi Optimization LLC, "Gurobi optimizer reference manual," 2019, [Online]. Available: https://www.gurobi.com/documentation/8.1/refman/index.html
[61] I. Dunning, J. Huchette, and M. Lubin, "Jump: A modeling language for mathematical optimization," *SIAM Review*, vol. 59, no. 2, pp. 295-320, 2017.